RSC Advances

PAPER

View Article Online
View Journal | View Issue

Cite this: *RSC Adv.*, 2021, **11**, 9693

Conductive nanosheets produced by UV irradiation of a Ag nanoparticle monolayer at the air–water interface

Masashi Kuroiwa, Tatsuya Nishimura, Mizuki Matsukawa, Yoshiro Imura, Ke-Hsuan Wang and Takeshi Kawai *

Received 19th January 2021
Accepted 26th February 2021

DOI: 10.1039/d1ra00454a

rsc.li/rsc-advances

In a previous study, we demonstrated that conductive Au nanosheets can be prepared by UV irradiation of an Au nanoparticle monolayer spreading on water. In this study, we applied this UV irradiation technique to inexpensive Ag nanoparticles (NPs) to expand their versatility. UV irradiation of Ag NPs on water resulted in the formation of large Ag NPs and was ineffective for preparing conductive Ag films. The solubilization of additives in the water phase, however, resulted in the conversion of the large Ag NPs into a nanosheet, and the solubilization method was highly effective for preparing transparent conductive Ag films with an optical transmittance of above 70%.

1. Introduction

Transparent conductive films are essential for manufacturing advanced optical and electronic devices.[1–7] Fluorine-doped tin oxide and indium-doped tin oxide films deposited *via* high-temperature processes are the most widely used transparent conductive films, although they are brittle against bending.[8,9] Recently, noble metal nanoparticles (NPs) or one-dimensional ultrathin nanowires (NWs)[10–12] have become the focus of research attention as fundamental materials for promising conductive films.[2–4,13] Researchers have reported that metal NP or NW arrays with grid pattern structures on proper substrates give rise to transparent conductive films.[3,4,14] To afford a high conductivity to such systems, however, the insulating organic compounds that cover them must be removed by O_2 plasma treatment or high-temperature annealing.[2,3,14] Furthermore, the area between the grid lines of the metal NPs is non-conductive. This area can be reduced by increasing the density of the grid lines; however, this comes with some disadvantages such as lower transparency and increased metal consumption.

Although thermal evaporation or electron beam deposition techniques are an alternative means of depositing ultrathin metal nanosheets on substrates, the manufacturing of homogenous ultrathin films of several nanometers in thickness is still a challenging task.[15] Furthermore, separating ultrathin metal films from the deposition substrates is generally difficult because of the strong adhesive force between the two, which practically prevents the transfer of the films to other suitable substrates.

Department of Industrial Chemistry, Tokyo University of Science, 1-3 Kagurazaka, Shinjuku-ku, Tokyo 162-8601, Japan. E-mail: kawai@ci.tus.ac.jp

The grid-pattern technique, as described above, has the inevitable disadvantage of requiring post-treatment to achieve electrical connection between the metal NPs; however, the development of metal NP-based fabrication methods for transparent conductive films still constitutes a viable pathway as we can easily access various synthesis protocols of metal NPs of desired sizes. An alternative candidate for the metal NP-based method is the transformation of metal NPs into nanosheets, which exhibit electrical conductivity in addition to sufficiently high transparency, flexibility, and a weak plasmonic band in the visible region.

In a previous study,[16] we proposed a new method for fabricating ultrathin Au nanosheets by UV irradiation of Au NP monolayers at the air–water interface. UV irradiation facilitated the decomposition and detachment of ligand molecules covering the Au NPs and promoted the transformation of the Au NPs into a nanosheet. We also demonstrated that the Au nanosheets can serve as ultrathin conductive films with high flexibility and transparency. In this work, to demonstrate the versatility of the UV irradiation method, we apply this technique to inexpensive Ag NPs covered with different ligand molecules. Furthermore, we demonstrate that the solubilization of additives in the water phase is highly effective for the morphological control of UV-irradiated objects produced from the original Ag NPs, and it leads to the transformation of Ag NPs into conductive Ag nanosheets.

2. Materials and methods

2.1 Materials

Sodium acetate (NaAc), silver nitrate, and oleylamine (OAm) were obtained from Kanto Chemical Co., Inc. Myristic acid (MyA), ethylenediamine tetraacetic acid disodium dihydrate (EDTA), tetraoctylammonium bromide (TOAB), and polyvinylpyrrolidone (PVP, molecular weight: 40 000 Da) were purchased from Tokyo

Chemical Industry Co., Ltd. Sodium oxalate (NaOx) was obtained from Wako Pure Chemical Industries, Ltd., and dodecanethiol (DDT) was obtained from Sigma-Aldrich. Prior to use, chloroform was distilled once to remove any impurities.

2.2 Preparation of DDT-, MyA- and OAm-capped Ag NP

Ag NPs capped with DDT were prepared according to a previously reported method with some modifications.[17] A 0.27 mmol $AgNO_3$ aqueous solution (9.0 mL) was added to 2.0 mmol of phase-transfer reagent, $(C_8H_{17})_4NBr$ (TOAB), dissolved in CCl_4 (8.9 mL), and the mixture was stirred for 15 min. The CCl_4 phase was subsequently collected, and 0.25 mmol DDT was added. After stirring for 15 min, a 3.1 mmol solution of sodium borohydride in water (7 mL) was added to reduce the Ag ions. The reaction mixture was vigorously stirred for 12 h to allow the formation of the Ag NPs. To remove excess DDT and TOAB, the as-prepared Ag NPs were washed thoroughly several times with acetone through centrifugal separation. The purified Ag NPs were dispersed in chloroform (5 mL).

MyA-capped and OAm-capped Ag NPs were then synthesized according to previous reports.[18,19] To remove excess MyA or OAm, the as-prepared Ag NPs were washed thoroughly with ethanol through several centrifugal separation cycles. The purified Ag NPs were dispersed in chloroform (5 mL).

2.3 Preparation of ultrathin Ag nanosheets

The suspension of purified Ag NPs in chloroform was spread on the surface of water or an aqueous solution of NaAc, NaOx, EDTA, or PVP, and compressed using a Teflon barrier up to a close-packed structure of Ag NPs. The sample was then irradiated with 248 nm UV light at an intensity of ~60 mW cm^{-2} using an optical fiber. The UV light source was a 250 W mercury lamp (REX-250, Asahi Spectra Co., Ltd.), and the wavelength of 248 nm was selected by narrow-band optical filters.

2.4 Characterization

The Ag nanosheets prepared at the air–water interface were gathered using various substrates: a copper grid coated with an elastic carbon film for transmission electron microscopy (TEM) observations; a CaF_2 substrate for Fourier transform infrared (FT-IR) spectroscopy measurements; and a quartz plate for UV-vis measurements. TEM was performed using a JEOL JEM-1011 microscope operating at 100 kV, while high-resolution TEM (HRTEM) and selected area electron diffraction (SAED) images were obtained with a JEM-2100 (JEOL) operated at 200 kV. UV-vis and FT-IR spectra were acquired using a UV-vis spectrometer (JASCO, V-570) and an FT-IR spectrophotometer (Thermo Scientific, Nicolet 6700), respectively. The electrical resistances of the Ag nanosheets deposited on SiO_2 plates were measured using the four-probe method with a Keithley 2400 source meter; the spacing between the adjacent probes was 1 mm.

3. Results and discussion

A monolayer of DDT-capped Ag NPs (6.0 ± 3.0 nm) was prepared by spreading the chloroform dispersion on water. The NP monolayer was irradiated with 248 nm UV light (60 mW cm^{-2}) through an optical fiber. Fig. 1 shows the morphological changes as a function of the duration of UV irradiation: a short irradiation time (1 min) resulted in the fusion of a few original NPs, and continuous irradiation for 20 min advanced the fusion and resulted in the formation of larger NPs. The mechanism promoting NP fusion lies in the decomposition of the DDT covering the Ag NPs.[16,20–22] More precisely, DDT decomposition may produce energetically unstable Ag NP bare surfaces, leading to NP agglomeration.[23] The decomposition is confirmed by the FT-IR spectra in Fig. 2, where the absorbance of the C–H stretching bands of DDT on Ag NPs clearly decreases with increasing irradiation time.

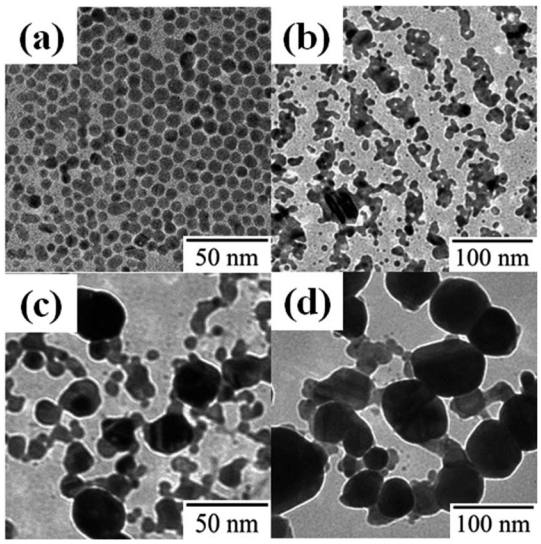

Fig. 1 TEM images of DDT-capped Ag NPs (a) before and after UV irradiation for (b) 1 min, (c) 10 min, and (d) 20 min.

Fig. 3a and b show the HRTEM images of large Ag NPs produced by UV irradiation times of 1 and 20 min, respectively. The first, in Fig. 3a, exhibited periodical fringes with different growth directions, indicating a polycrystalline structure consisting of an aggregate of several original Ag NPs. On the other hand, the sample irradiated for 20 min (Fig. 3b) showed a single-direction periodical fringe. To gather more detailed

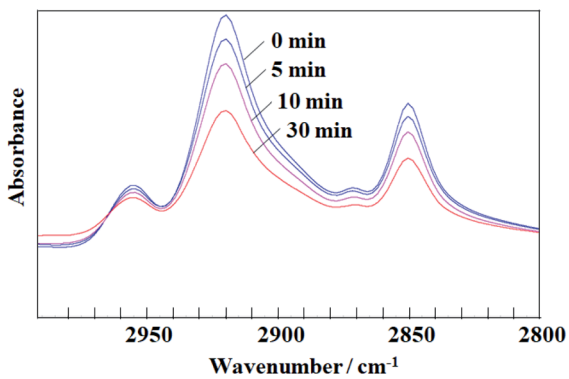

Fig. 2 FT-IR spectra of a DDT-capped Ag NP monolayer in the C–H stretching region before and after UV irradiation for 5, 10, and 20 min.

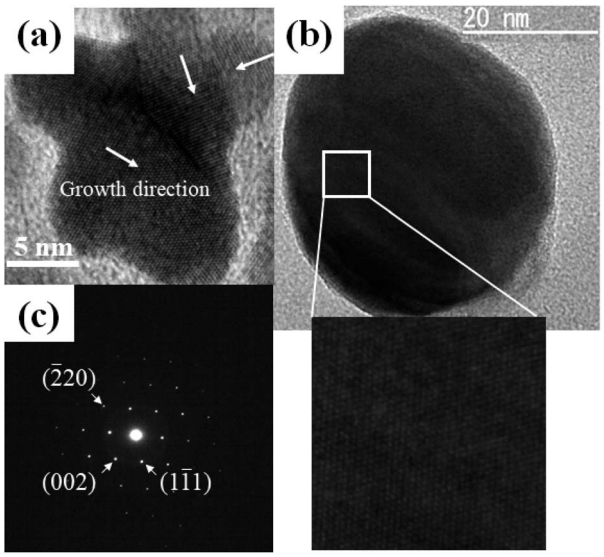

Fig. 3 HRTEM images of DDT-capped Ag NPs after UV irradiation for (a) 1 min and (b) 20 min; (c) SAED pattern of 20 min UV irradiated Ag NP.

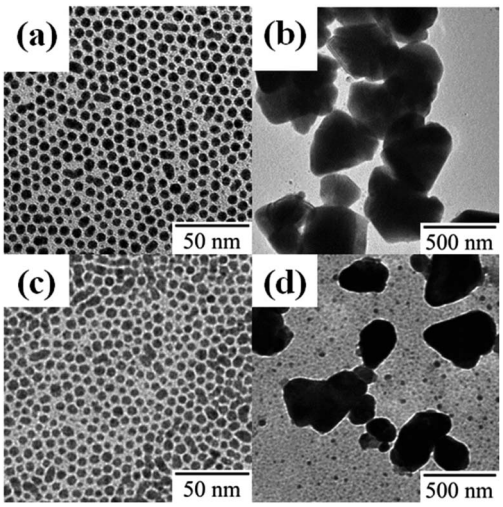

Fig. 4 TEM images of (a and b) MyA- and (c and d) OAm-capped Ag NPs (a and c) before and (b and d) after UV irradiation for 10 min.

data on the fringe, the SAED pattern of the Ag NP was then observed: Fig. 3c clearly shows diffraction spots originating from a single crystal domain, which correspond to the fringe spacings of 0.14, 0.20 and 0.24 nm, assigned to the (220), (200), and (111) reflections of metallic Ag, respectively.[24,25] Accordingly, we can conclude that UV irradiation determined the fusion of the original Ag NPs. In addition, as no spots in Fig. 3c could be assigned to silver oxide, we can deduce that the Ag NPs were not oxidized by UV irradiation.

Unfortunately, the large NP aggregates in Fig. 1d did not exhibit any electrical conductivity, which was in contrast with previously reported Au nanosheets prepared from Au NPs using the same UV irradiation method.[16] The absence of conductivity is most likely correlated with the morphology of the aggregates. The reason why large Ag NPs, instead of a nanosheet, are formed following UV irradiation is not sufficiently understood so far, but the difference between Au NPs and Ag NPs is possibly related to the difference in wettability or solid-state de-wetting behavior.[26–28] The evaluation of the differences in the properties and behaviors of the two systems is not straightforward owing to the absence of data on the precise surface structure, adsorbed species, and compositions of the NPs.

In view of these findings, one could hypothesize that the surface modification of Ag NPs may allow control of the morphology of UV-irradiated Ag nanocrystals. The simplest way to modify the Ag NP surface is the use of different ligand molecules. Thus, MyA-capped Ag NPs (5.6 ± 0.7 nm) and OAm-capped Ag NPs (5.8 ± 1.4 nm) were synthesized, and the particles were spread on water (Fig. 4a and c) and subjected to UV irradiation. Contrary to our expectations, in both instances large NPs were obtained (Fig. 4b and d), similar to the product obtained from DDT-capped Ag NPs.

Evidently, the ligand molecules had little influence on the morphology of the final products. A possible reason might be an incomplete capping of the NP surface; during the transformation from the original NP into nanocrystals of different shapes and/or in the process of decomposition of ligand molecules by UV irradiation, sufficient ligand molecules were not present to cover the newly emerged crystal surfaces. One way to overcome this problem is to add silver-absorbable compounds into the water phase. NaAc, NaOx, and EDTA were selected as the additives because the carboxylate group is preferentially adsorbed on the (111) facet of Ag.[29] Furthermore, PVP was also used as an additive because PVP binds strongly to Ag(100).[24,30] Next, DDT-capped Ag NP monolayers were prepared on the surface of aqueous solutions of these additives and then subjected to UV irradiation. Fig. 5 shows TEM images of Ag NP monolayers on (a) NaAc (50 mM), (b) NaOx (26 mM), (c) EDTA (27 mM), and (d) PVP (0.15 wt%) solutions after UV irradiation. The products formed on NaOx, EDTA, and PVP solutions exhibited mesh-like structures, whereas those on the NaAc solution were large Ag NPs similar to the product obtained on pure water. Fig. 5e shows HRTEM image of DDT-capped Ag NPs on PVP after UV irradiation. Periodical fringes with different directions prove that the mesh-like nanosheets have a polycrystalline structure, indicating that the fusion of Ag NPs progresses gently. Since the spacing of the periodical fringes was 0.24 nm corresponding to the lattice spacing of Ag(111), the mesh-like products were metallic Ag.

Fig. 6 depicts a schematic illustration of the possible mechanism for the effect of the additives on the morphology of Ag NPs. Without the additives (Fig. 6a–c), the photodecomposition of the ligand molecules covering Ag NPs causes aggregation and fusion of Ag NPs. Prolonged UV irradiation results in a considerable decomposition of the ligand molecules deposited on the whole surface of Ag NPs. Since the bare surface of Ag NPs is energetically unstable, the aggregation and fusion of Ag NPs may occur in all directions, leading to a formation of large Ag NPs (Fig. 6c).

In case of the aqueous solutions of silver-absorbable additives (Fig. 6d–f), when the ligand molecules covering Ag NPs are

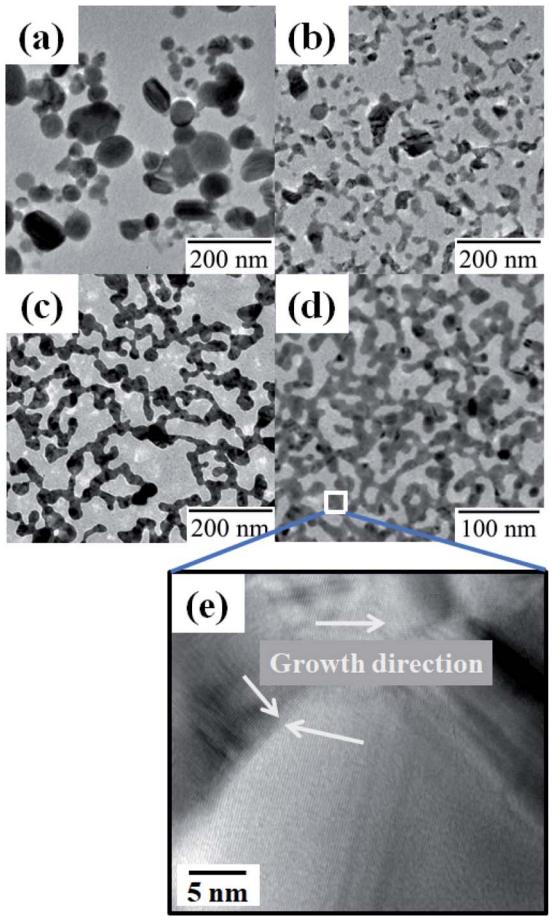

Fig. 5 TEM images of DDT-capped Ag NPs on (a) NaAc, (b) NaOx, (c) EDTA, and (d) PVP, and (e) HRTEM image of DDT-capped Ag NPs on PVP after UV irradiation.

decomposed by UV irradiation, the additives should be adsorb on the bottom surface of Ag NPs (Fig. 6e). Aggregation and fusion between the additive-adsorbed surfaces are likely suppressed due to the electrostatic repulsion between COO^- groups of EDTA and NaOx or steric repulsion between adsorbed PVP polymer chains. On the other hand, ligand-free side faces of Ag NPs, which are energetically unstable bare surface, promote connections between the Ag NPs, resulting in the formation of percolated network structure of Ag NPs. Here, the adsorbed additives may be decomposed by UV irradiation, but new additive molecules are plentifully supplied from the bulk water phase. Consequently, the adsorption layer of the additives on the bottom of Ag NPs effectively prevents three dimensional aggregation of the Ag NPs.

As anticipated, the addition of suitable additives to water is a highly effective means for changing the morphology of Ag nanocrystals. The as-prepared Ag films were transferred on SiO_2 plates, and their electrical resistances were measured using the four-probe method. The measured electrical resistances were 104 kΩ for NaOx, 0.37 kΩ for EDTA, and 1.6 kΩ for PVP, indicating that the mesh-like films had a percolated network structure extending across the entire area of the monolayer exposed to UV light (several tens of mm^2). Here, the deviation in the electrical resistances of the NaOx films was large, ranging from several hundred to several thousand Ω. This was possibly because of the many disconnections in the network structure, as shown in Fig. 5b.

Fig. 7 presents the UV-vis spectra of the original Ag NPs and the highest conductive Ag nanosheet produced on EDTA. UV irradiation resulted in the weakening of the plasmon band of Ag NPs at ~500 nm, and the transmittance of the nanosheet was above 70% in the visible region. Because the previously reported Au nanosheets had an electrical resistance of 0.15 kΩ and an optical transmittance of ~80%,[16] the performance of the present Ag nanosheet was roughly comparable to that of Au nanosheets, suggesting that the combination of the present UV irradiation method and additives in the water phase is generally effective for fabricating metal nanosheets from the corresponding NPs. Since the present performance was surely a little

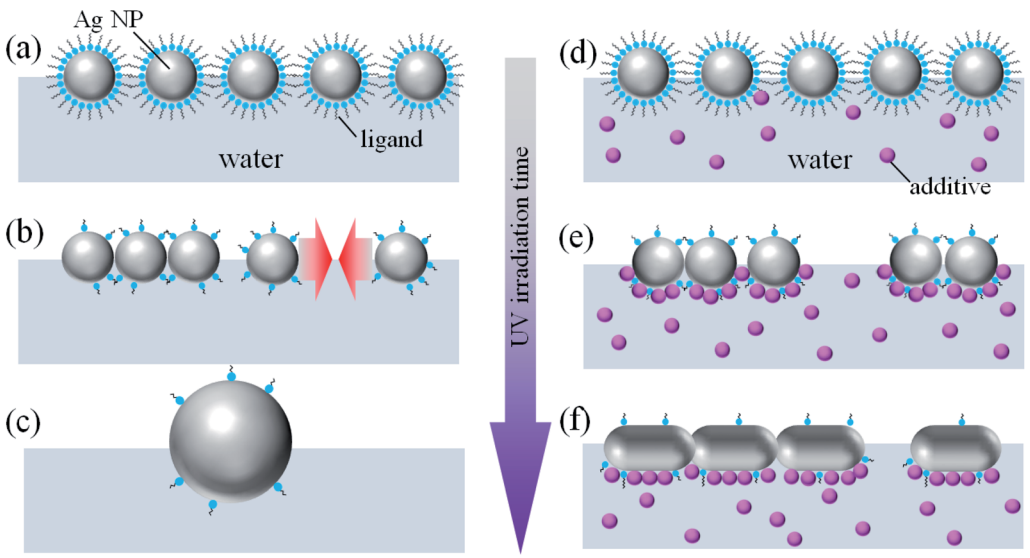

Fig. 6 A schematic illustration of the effect of the additives on the morphology of Ag NPs.

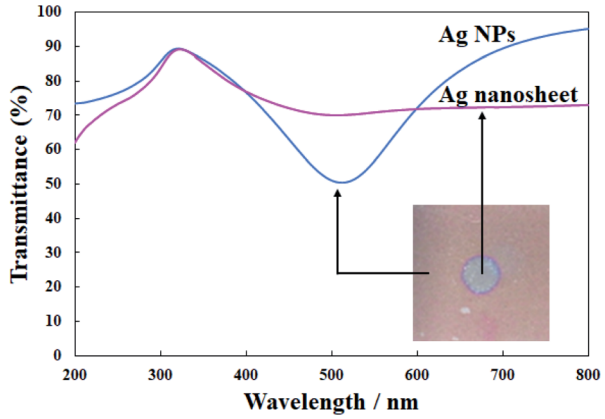

Fig. 7 Transmittance of Ag NP monolayer and UV-irradiated Ag nanosheet. The irradiation time of UV light was 10 min. Photograph of Ag NP monolayer deposited on SiO_2 after irradiation. The center and surrounding areas are the irradiated and non-irradiated parts, respectively.

lower than that of the Au nanosheet, to achieve the best performance, further investigation of the effects of the Ag NP diameter, other additives, and their concentrations is required, which might be the object of future work.

4. Conclusions

In summary, the UV irradiation method was applied to inexpensive Ag NP monolayers at the air–water interface. The method was sufficiently promising for producing electrically conductive Ag nanosheets, even though some modifications are required to improve their conductivity. The morphology of UV-irradiated Ag nanocrystals was practically independent of the type of ligand covering the Ag NPs, whereas it was influenced by additives in the water phase. The additives EDTA, PVP, and NaOx in water were highly effective for preparing conductive Ag nanosheets.

Conflicts of interest

The authors declare no conflicts of interest.

Acknowledgements

This work was supported in part by JSPS KAKENHI Grant Numbers 19H02538 and 19K22116.

References

1 D. Azulai, T. Belenkova, H. Gilon, Z. Barkay and G. Markovich, *Nano Lett.*, 2009, **9**, 4246.
2 A. Morag, L. Philosof-Mazor, R. Volinsky, E. Mentovich, S. Richter and R. Jelinek, *Adv. Mater.*, 2011, **23**, 4327.
3 K. Higashitani, C. E. McNamee and M. Nakayama, *Langmuir*, 2011, **27**, 2080.
4 T. Kister, J. H. M. Maurer, L. González-García and T. Kraus, *ACS Appl. Mater. Interfaces*, 2018, **10**, 6079.
5 J. van de Groep, P. Spinelli and A. Polman, *Nano Lett.*, 2012, **12**, 3138.
6 Y. Chen, Z. Ouyang, M. Gu and W. Cheng, *Adv. Mater.*, 2013, **25**, 80.
7 S. Gong, Y. Zhao, L. W. Yap, Q. Shi, Y. Wang, J. A. P. B. Bay, D. T. H. Lai, H. Uddin and W. Cheng, *Adv. Electron. Mater.*, 2016, **2**, 1600121.
8 D. P. Tran, H. I. Lu and C. K. Lin, *Coating*, 2018, **8**, 212.
9 L. Hu, D. S. Hecht and G. Grüner, *Chem. Rev.*, 2010, **110**, 5790.
10 R. Takahata, S. Yamazoe, K. Koyasu and T. Tsukuda, *J. Am. Chem. Soc.*, 2014, **136**, 8489.
11 M. Nakagawa and T. Kawai, *J. Am. Chem. Soc.*, 2018, **140**, 4991.
12 N. Miyajima, Y.-C. Wang, M. Nakagawa, H. Kurata, Y. Imura, K.-H. Wang and T. Kawai, *Bull. Chem. Soc. Jpn.*, 2020, **93**, 1372.
13 Y. Kim, J. Zhu, B. Yeom, M. Di Prima, X. Su, J.-G. Kim, S. J. Yoo, C. Uher and N. A. Kotov, *Nature*, 2013, **500**, 59.
14 Y. He, Y. Chen, Q. Xu, J. Xu and J. Weng, *ACS Appl. Mater. Interfaces*, 2017, **9**, 7826.
15 Y. G. Bi, Y. F. Liu, X. L. Zhang, D. Yin, W. Q. Wang, J. Feng and H. B. Sun, *Adv. Opt. Mater.*, 2019, **7**, 1800778.
16 T. Nishimura, N. Ito, K. Kinoshita, M. Matsukawa, Y. Imura and T. Kawai, *Small*, 2020, **16**, 1903365.
17 M. Brust, M. Walker, D. Bethell, D. J. Schiffrin and R. Whyman, *J. Chem. Soc., Chem. Commun.*, 1994, 801.
18 M. Yamamoto and M. Nakamoto, *J. Mater. Chem.*, 2003, **13**, 2064.
19 M. Chen, Y.-G. Feng, X. Wang, T.-C. Li, J.-Y. Zhang and D.-J. Qian, *Langmuir*, 2007, **23**, 5296.
20 N. J. Brewer, R. E. Rawsterne, S. Kothari and G. J. Leggett, *J. Am. Chem. Soc.*, 2001, **123**, 4089.
21 S. Sun, K. S. L. Chong and G. J. Leggett, *J. Am. Chem. Soc.*, 2002, **124**, 2414.
22 R. E. Ducker, S. Janusz, S. Sun and G. J. Leggett, *J. Am. Chem. Soc.*, 2007, **129**, 14842.
23 H. Lu, D. Zhang, X. Ren, J. Liu and W. C. H. Choy, *Nano Lett.*, 2014, **8**, 10980.
24 J. Zeng, Y. Zheng, M. Rycenga, J. Tao, Z.-Y. Li, Q. Zhang, Y. Zhu and Y. Xia, *J. Am. Chem. Soc.*, 2010, **132**, 8552.
25 V. Germain, J. Li, D. Ingert, Z. L. Wang and M. P. Pileni, *J. Phys. Chem. B*, 2003, **107**, 8717.
26 H. Oh, A. Pyatenko and M. Lee, *Appl. Surf. Sci.*, 2019, **475**, 740.
27 A. Araújo, M. J. Mendes, T. Mateus, A. Vicente, D. Nunes, T. Calmeiro, E. Fortunato, H. Águas and R. Martins, *J. Phys. Chem. C*, 2016, **120**, 18235.
28 C. V. Thompson, *Annu. Rev. Mater. Res.*, 2012, **42**, 399.
29 Z. Tang, Q. Zhang, Y. Yin and C. A. Chang, *J. Phys. Chem. C*, 2014, **118**, 21589.
30 W. A. Al-Saidi, H. Feng and K. A. Fichthorn, *Nano Lett.*, 2012, **12**, 997.